38th International Electric Vehicle Symposium and Exhibition (EVS38)
Göteborg, Sweden, June 15-18, 2025

Impact of External Pressure on the Performance Characteristics of Commercial Lithium-Ion Cells along their Cycle Life

Ander Avila[1,2,*], Adrián Remirez[1], Eduardo Miguel[1], Laura Carreras[2], Pere Maimí[2]
[1]*Ikerlan Technology Research Centre, Basque Research and Technology Alliance (BRTA), Arrasate-Mondragon, Spain*
[2]*AMADE - Analysis and Advanced Materials for Structural Design, Universitat de Girona, Campus Montlivi, Edif. PII, 17003 Girona, Catalonia, Spain*
[*]*Corresponding author: ander.avila@ikerlan.es*

Executive Summary

This study investigates the role of external mechanical pressure on the performance of commercial prismatic lithium-ion cells across their lifecycle, comparing pristine and aged NMC/Gr cells. The research demonstrates that pressure significantly influences key electrochemical and mechanical behaviours, especially in aged cells. Applied pressure enhances discharge capacity (up to 2.88% in aged cells) and reduces impedance (41.3% DCR reduction), improving internal conductivity and reaction kinetics. Swelling measurements reveal aged cells exhibit lower mechanical stiffness at low pressures due to gas accumulation, which is mitigated under higher pressure, restoring structural integrity. Analysis of phase transition voltages suggests an optimal pressure ($\sim$ 0.2 MPa) for enhancing anode kinetics in pristine cells. Resistance gradient trends further confirm improved interfacial contact and reduced kinetic resistance under pressure. Overall, the findings highlight that external pressure can be strategically tuned, not only for structural purposes, but as a functional parameter to enhance cell performance and longevity.

Keywords: Batteries, Packing, Cooling & Heat Transfer, Modelling & Simulation, Life Cycle Analysis, Battery Manufacturing

1 Introduction

Lithium-ion batteries (LIBs) have transformed our world by storing energy efficiently and making it available whenever needed. Initially, they were used only in small devices such as cell phones, laptops, and other similar electronics with minimal requirements. Later, however, they were adopted in renewable energy storage systems and electric/hybrid vehicles, which operate under much harsher conditions [1]. This shift highlighted the importance of gaining deeper insight into understanding the complex relationship between battery performance and environmental conditions.

Battery cells are integrated into modules or packs with the requested thermal management, control units, and buffer elements. Prismatic and pouch cells are assembled under applied stack pressure and secured using various clamping strategies, such as welding or mechanical joining. Cylindrical cells, on the other hand, are typically arranged in a staggered pattern, which minimizes volume loss due to their shape.

These assemblies are then mounted on the application [2, 3]. As a result, LIBs usually operate under different temperatures, charge/discharge rates, initial mechanical pressure conditions, and mechanical constraints, which influences the electrical performance and degradation rate of the battery [4]. Previous studies have analysed the role of these conditions in commercial batteries, as well as their interaction, along their lifespan.

The impact of temperature on the operation of lithium-ion batteries has been thoroughly studied and analyzed in the literature. Lv et al. [5] studied the effect of the temperature range from -40°C to 60°C in the discharge capacity at 1C of LCO, LFP and LMO battery cells, showing a decrease in discharge capacity with the decrease from the standard temperature of 88.3%, 53.4% and 63.2% respectively; and a maximum change of -2.3%, 10.9% and 23.5% respectively with higher temperatures. Leng et al. [6] show the same effect in LCO battery cells while they age, as well as the battery degradation speeds up at high temperatures. Temperature also influences battery impedance, decreasing with increasing temperature [7, 8]. These two effects can be considered as coupled, as the resistance decreases, the capacity increases in characterization tests.

To accelerate charging times in the industry and address range anxiety, it is essential to focus on the effects of battery charge and discharge rates. Wang et al. [9] analysed discharge rates between 1C and 11C in cylindrical ternary batteries, showing a decrease in discharge capacity with increasing current in the process, from 86.45% of nominal capacity to 78.42%. Similar tendencies are seen in other chemistries such as LFP [10, 11] or LCO [12]. Minimum effects are considered in the impedance spectra influenced by the current rate [5, 13, 14, 15]. Wang et al. [21] analysed the interplay between an ambient temperature range of -5°C to 40°C and a current rate from 0.1C to 1C in commercial prismatic NMC cells. The maximum change in discharge capacity due to current is not greater than 5% of the nominal capacity, and the battery only reaches the nominal capacity with temperatures above 10°C. At -20°C the battery only remains the 80% of its nominal capacity, explained mainly by the increase in the electrolyte viscosity, which shows serious polarization, and the decrease in diffusion coefficient that increases the charge transfer resistance [5]. Xu et al. [16] study the response of LCO-NCA blended cathode pouch cells at different C rates throughout their lifetime, concluding that the C rate influence is greater in aged batteries, as their resistance is greater and the thermal effects increase.

Finally, the influence of external pressure over the battery due to the assembly is also important to understand. Du et al. [17] analyse the performance of commercial NMC/Gr pouch cells in a stack pressure range of 30 kPa to 310 kPa. They found that pressure had no significant effect on discharge capacity at current rates between C/3 and 2C; however, differences in impedance are shown. Increasing pressure improves electrode contact and reduces charge transport distance, reducing ohmic and charge transfer resistances. However, it increases the resistance of the SEI, indicating structural changes in the SEI layer. Muller et al. [18] did a similar study with laboratory pouch cells with same results in impedances, but, they determined that the pressure improves battery discharge capacity at low C rates, and impairs in higher ones. Y. Jiang et al. [18] used NMC and LFP pouch cells to analyze the change between 0-0.2 MPa of the open-circuit voltage (OCV) and impedance in the cell. The maximum OCV difference caused by stack pressure in NMC cells and LFP cells is 12.1 mV and 4.3 mV, respectively. Ohmic resistance also changes up to 30.9% on the NMC cell. Zhou et al. [20] analysed the effects in NMC 28Ah pristine and 32Ah aged NMC pouch cells. The aged cell recovers 1.6% of discharge capacity after applying 1 MPa pressure, while the pristine cells do not have significant change. Nevertheless, the direct current resistance (DCR) of the pristine cells decreases in 13.7% with 1 MPa, while in aged cell it has no significant effects. Xue Cai et al. [22] analyzed the coupling between the mechanical, thermal and electrical behaviour of a NCM811 pristine commercial pouch cells with Gr-SiOx anode considering temperature, state of charge (SoC), external pressure, and current rate. The external pressure influences the DCR of the cell with different tendencies depending on the temperature. At 10°C a decrease of 44.8% is observed, while at 40°C an increase of 6.3% is shown. This effect is related to the increase in the contact area between the electrode layer and the current collectors, while at 40°C the narrower separator pathways and blocked ion diffusion paths caused by pressure are the primary factors contributing to the increased resistance. An inverse trend is seen in the discharge capacity, where the capacity increases in 8% at 10°C and decreases 1.5% at 40°C.

The influence of mechanical pressure on battery performance is analysed in the literature as aforementioned, but a lack of comprehension is identified throughout cell lifetime. Different pressures are analysed in pristine cells, but not in aged ones, except from Zhou et al. [20], but they did it with different battery cells. There is a great deal of literature [23, 24, 25, 26, 27] in which cells are aged at different stack pressures and then they are analysed, but in this cases different state of healths (SoHs) are not considered.

This study focuses in the analysis of the influence of different stack pressures in a pristine and aged prismatic cell, in order to analyse whether pressure has different effects at different points of cell's lifetime.

2 Case of study

2.1 Battery cell

The study is carried out in commercial prismatic cells with a nominal capacity of 58Ah, a voltage range of 2.75 to 4.35V and an operating temperature of -20 to 55 °C. The cells are comprised of the cathode of NCM and anode of graphite. A more detailed description of the battery cells is summarized in Table 1. The aged cell was subjected to 1520 cycles under controlled conditions designed to accelerate degradation. The cell was operated without any external stack pressure, at an ambient temperature of 45 °C. Charge and discharge were performed at a constant current of C/3, using a depth of discharge of 80%, centered around a 50% SoC.

Table 1: Specifications of the battery cells used in this study

Specifications	Sample
Cathode materials	NMC
Anode materials	Gr
Nominal capacity (Ah)	58
Voltage range (V)	2.75-4.35
Temperature (°C)	-20 - 50
Cell dimension (Length × width × height) (mm)	148.2 × 105.9 × 26.7
Maximum charge /discharge rate (C/C)	1.2/1
Weight (g)	926

2.2 Set-up

The battery cells are tested within a pressure set-up, which consists of two movable plates within a fixed structure made up of four structural rods and four guides. The movable plates are free to move on the guides due to 4 bearings with negligible frictional force. A load cell (Utilcell, 420-5t, Spain) is located under one movable plate in order to measure the applied force over the cell. The cell is positioned between the movable plates and then the force is applied with a spindle with thin thread on the second movable plate. Then a type K thermocouple is positioned on the side of the cell to measure its temperature. This set-up is placed within a temperature controllable chamber (CTS, T-40/2000/LI, Germany). The thermocouple is connected to a temperature data logger (Digatron, DLT-16, Germany), and then the battery cell and the data logger are connected to the cycler (Digatron, MCT-ME, Germany) which powers the cell and measures its voltage and temperature. The cell terminals are joined using mechanical fastening, consisting of a stainless steel spring washer and an M6 nut tightened to a torque of 2 N·m. The acquisition of the force is done with an independent data logger (Agilent, 34972A, USA). The representation of the whole set-up can be seen in Fig. 1. The sample rate of the cycler is defined as 1 Hz, and for the pressure 0.1 Hz.

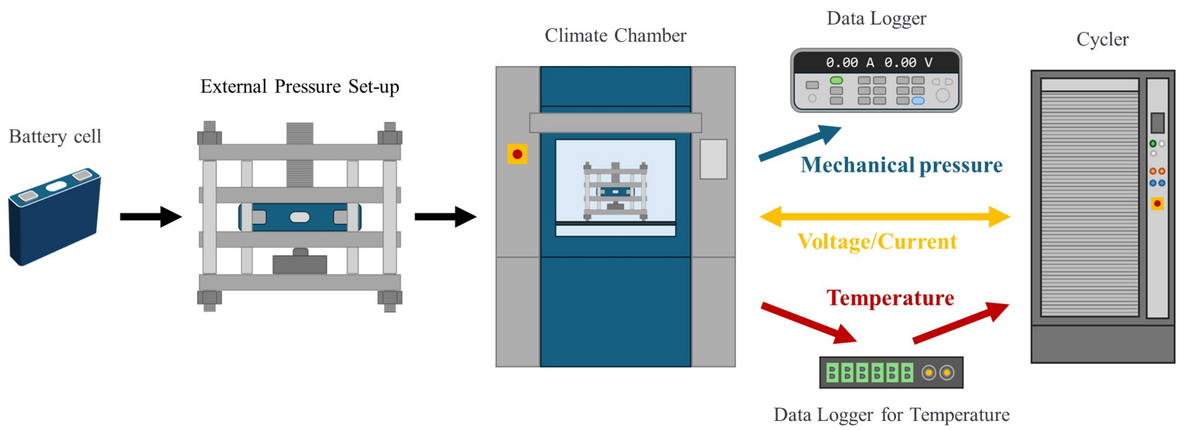

Figure 1: Representation of the experimental set up.

3 Testing procedure

In this section the characterization tests carried out with every condition are defined. The tests are carried out at an ambient temperature of 25 °C. The external pressure applied over the cell are 0 MPa, 0.05 MPa, 0.2 MPa, and 1 MPa. The pressure is applied when the cell has a SoC of 20%. The experiments carried out in the study can be seen in Table 2, which are preconditioning tests, capacity tests, quasi-open circuit voltage (qOCV) test, and high power pulse characterization (HPPC) tests.

Table 2: Experimental matrix for pristine and aged cell.

Experiments	SoC (%)	C-rate (C)	Pressure (MPa)	Ambient temperature (°C)
Preconditioning	-	1	0	25
Capacity			0 0.05, 0.2, 1	
qOCV		1/25		
HPPC	0-100	1/5, 1/3, 1/2, 1		

3.1 Preconditioning test

Both cells were stored for a long time before the tests, so some preconditioning tests were carried out to stable initial conditions. The cells were cycled 5 times at 1C/1C, with CC-CV method in charge, CC in discharge and 30 minute pauses between each step. This test is only done once and then the characterization tests are carried out.

3.2 Capacity test

The capacity tests are carried out with the same charge/discharge method as the preconditioning test, at 1CC-CV/1CC. The cell is fully charged and then the discharge capacity of the cell is measured, which is considered the remaining capacity of the cell. Finally, the cell is fully charged again for the next characterization tests.

3.3 qOCV test

The qOCV test is carried out to check the effect of pressure on the equilibrium voltage of the cell when the charge/discharge rate is so low that the thermal effects due to the impedance are negligible. It is assumed that the measured voltage in this test is the OCV. The cell is charged and discharged at a constant current of C/25 with pauses of 30 minutes between steps. This test starts after the full charge of the capacity test, so the cell is first discharged and then charged.

3.4 HPPC test

An HPPC test is performed to evaluate the cell's impedance across a wide range of SoC. This test is conducted from 100% to 0% SoC using a combination of charge and discharge current pulses at increasing C-rates (C/5, C/3, C/2, and 1C).

The procedure begins with a fully charged cell, immediately following the qOCV test. A sequence of 30 second charge and discharge pulses is applied at each C rate, in ascending order. After each pulse, a 5 minute rest period is introduced to allow the cell to stabilize. During the pulses, data is recorded at a sampling rate of 100 Hz to accurately capture voltage and current responses.

Once the full pulse sequence is completed at a given SoC level, the cell is discharged by 10% SOC at a constant rate of C/3 (e.g., from 100% to 90%). The pulse sequence is then repeated at the new SoC level. This cycle—pulse sequence followed by a 10% SoC discharge—is repeated incrementally until the cell reaches 0% SoC, enabling impedance measurements across the entire SoC range.

4 Results and discussions

The following sections present an analysis of the results obtained in this study. It begins with a discussion of the discharge capacity observed during the capacity tests. Then the OCV and swelling forces are analysed based on the qOCV measurents, paying atention to the differences in Incremental Capacity Analysis (ICA) and the Differential Pressure Analysis with respect to SoC (DPAQ). Finally, the change in the impedance of the battery is discussed with the results of the HPPC tests.

4.1 Discharge capacity

The discharge profiles are analyzed in the specified range of pressures in both cells. The extracted capacity is considered as a quantitative metric of performance, with higher values indicating enhanced electrochemical efficiency under the given conditions. As shown in Fig. 2, the effect of external pressure is more pronounced in aged cells compared to pristine ones. Specifically, the maximum enhancement in discharge capacity attributed to applied pressure is 0.46% in the pristine cell and 2.88% in the aged cell. Despite the differing magnitudes of influence, both cells exhibit a similar trend: discharge capacity increases with pressure, but approaches a plateau, indicating a saturation behaviour at higher pressure levels.

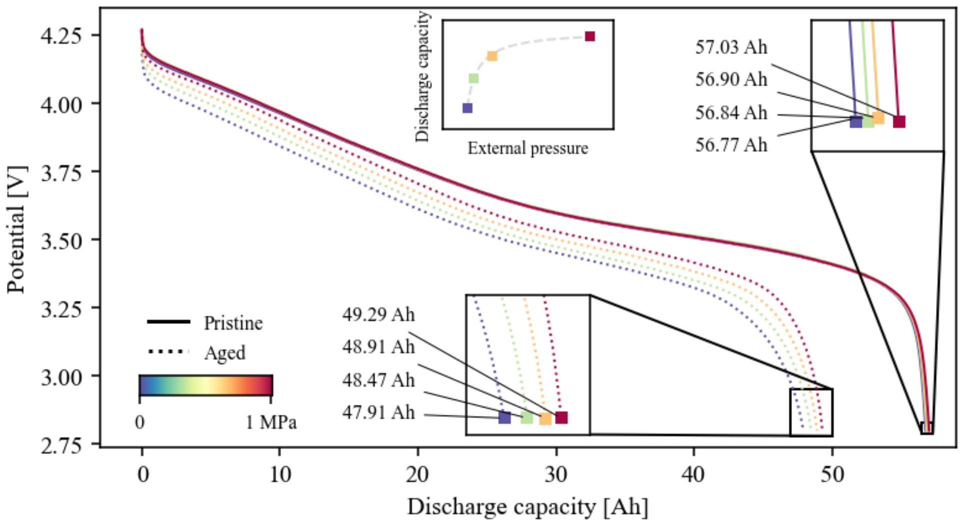

Figure 2: Discharge curves at different external pressures.

Since no active cooling system was integrated into the experimental setup and the cells were cycled at a 1C rate, potential thermal effects could influence the results. Fig. 3 presents the temperature profiles recorded during each test. For the pristine cell, temperature evolution appears to be consistent between tests, suggesting that thermal effects are negligible for comparative purposes. In contrast, the aged cell exhibits varying temperature profiles, particularly under applied pressures of 0 MPa and 1 MPa. These deviations are likely influenced by uncontrolled environmental factors within the climate chamber, potentially related to overlapping experimental activities or intermittent door openings. Nonetheless, as elevated temperatures are known to enhance discharge capacity [5], the observed pressure effects may be slightly underestimated.

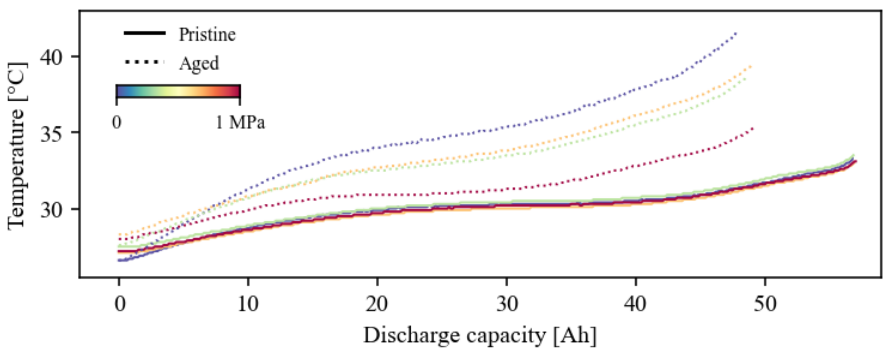

Figure 3: Temperature when the cells are discharged.

4.2 OCV and ICA

To better understand the cell's equilibrium voltage behaviour across different SoC we analysed the qOCV results. The use of very low current rates in this test minimizes the influence of polarization and internal resistance, providing a more accurate voltage–SoC profile that reflects the cell's underlying electrochemical characteristics. Throughout the qOCV measurements, the cell temperature was maintained at 25°C, with fluctuations limited to less than 1°C, ensuring limited thermal effects. Fig. 4 shows the qOCV curves for both cells. The effect previously seen in discharge capacity at 1C continues in the aged cell at low current rates, increasing 1.33% the capacity.

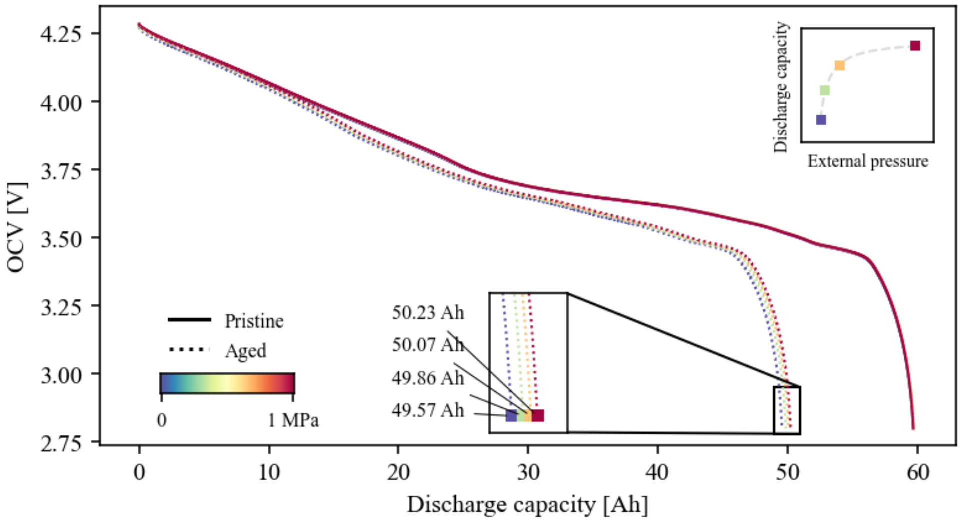

Figure 4: OCV curves at different external pressures.

To evaluate the cell's electrochemical behaviour, incremental capacity analysis (ICA) was performed, with the resulting dQ/dV curves shown in Fig. 5. Peaks at ~3.5 V (I and IV) and ~3.6 V (II and III) correspond to the graphite phase transition ($C_6 \rightarrow \mathrm{LiC}_x$) and the H_1–M transition in the NMC cathode, respectively [28]. While peaks II–III remain largely unaffected by pressure, the graphite-related peaks shift to lower voltages under compression. In pristine cells, this shift reaches a minimum near 0.2 MPa before increasing again, suggesting improved kinetics at moderate pressures. The aged cell, however, shows a continuous decrease in transition voltage with pressure up to 1 MPa, indicating a modified pressure response due to aging.

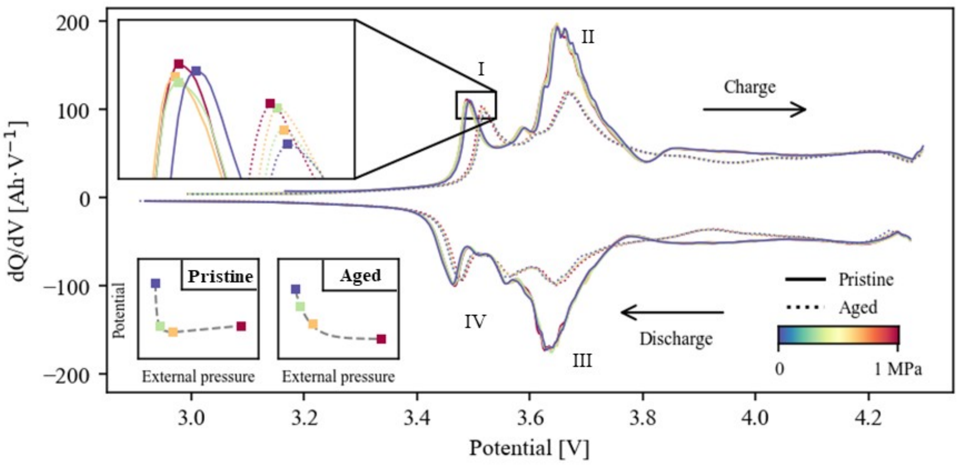

Figure 5: ICA with different external pressures.

4.3 Reversible swelling pressure

The analysis of reversible swelling pressure is conducted with the measurements under qOCV conditions to isolate the mechanical response associated purely with lithium diffusion. By employing very low current rates qOCV testing minimizes kinetic and thermal contributions, such as those arising from electrode heating or thermal strain. This approach enables the accurate measurement of swelling pressure induced solely by electrochemical intercalation and deintercalation processes.

Fig. 6a presents the absolute pressure recorded for each precompression level, while Fig. 6b illustrates the pressure variation relative to the initial stack pressure throughout the cycle. Pristine cells exhibited greater pressure changes compared to aged cells. Specifically, the maximum pressure differences observed in the pristine cell during a full cycle were 0.088 MPa, 0.094 MPa, and 0.128 MPa for initial stack pressures of 0.05 MPa, 0.2 MPa, and 1 MPa, respectively. In contrast, the aged cell displayed pressure variations of 0.032 MPa, 0.070 MPa, and 0.120 MPa under the same conditions. A linear relationship was observed between stack pressure and the maximum swelling pressure gradient in the pristine cell. The aged cell, however, exhibited a reduced initial pressure gradient at low stack pressures, indicating decreased stiffness. This softening effect is likely due to gas generation and accumulation within the cell, leading to irreversible swelling [29]. As the external pressure increases, these gases are displaced toward the edges of the cell, resulting in a more compact structure and a mechanical response that approaches that of the pristine cell.

To further examine the mechanical behaviour, the derivative of swelling pressure with respect to SoC was calculated in Fig. 6c. The pristine cell showed consistent behaviour across all stack pressure conditions, whereas the aged cell demonstrated increasing stiffness with higher external pressure, consistent with the previously described gas redistribution and compaction effects.

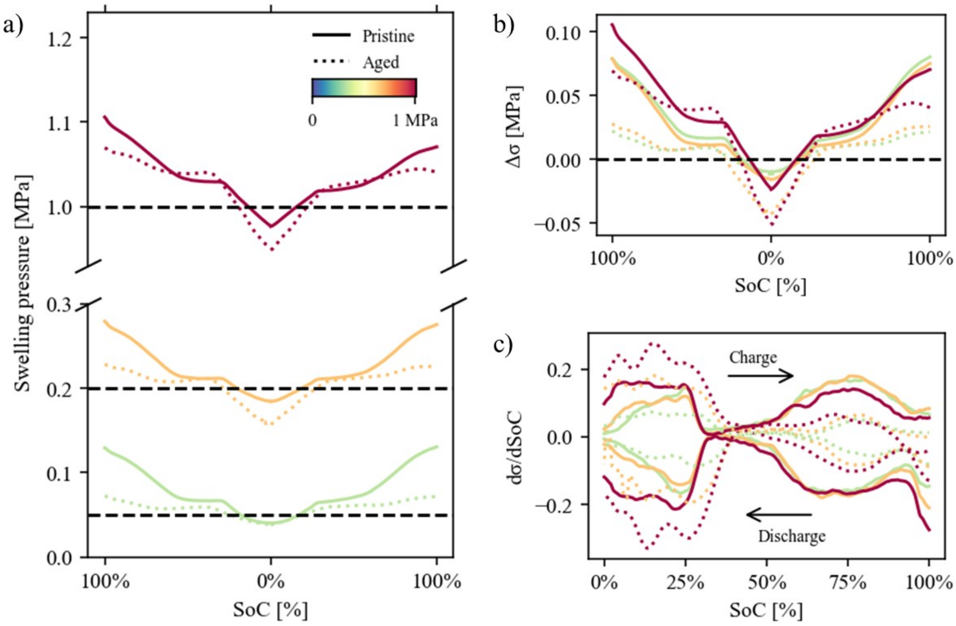

Figure 6: Mechanical response analysis with different initial stack pressures: a) Swelling force evolution. b) Pressure variation relative to the initial stack pressure throughout the cycle. c) DPAQ.

4.4 Impedance

Finally, the impedance data obtained from the HPPC test are analyzed to evaluate the cell's electrochemical performance across different SoCs, with a particular focus on the influence of external pressure. Fig.7a presents the measured resistance during the pulse at 20% SoC. A significant effect of stack pressure is observed in the aged cell: the ohmic resistance decreases by 41.3% when 1 MPa of pressure is applied. In contrast, the pristine cell exhibits a slight increase in resistance of 4.7% under the same conditions. This opposing trend in direct current resistance (DCR) with increasing pressure highlights a fundamental difference in the mechanical–electrochemical response of pristine and aged cells.

To further investigate the electrochemical kinetics, the resistance gradient—defined as the difference in DCR between the end and beginning of the pulse is presented in Fig. 7b. For aged cells, the resistance gradient follows a similar decreasing trend as the DCR with increasing pressure. This indicates that external pressure not only reduces the overall impedance but also improves the reaction kinetics during the pulse. Such behaviour suggests enhanced interfacial contact, contributing to improved performance. The associated decrease in Joule heating further supports the positive effect of pressure, consistent with the observed increases in discharge capacity.

In contrast, the pristine cell shows a non-monotonic trend: the resistance gradient decreases with pressure up to a certain point, after which it begins to increase. A similar behaviour was observed in the graphite intercalation peak voltage of the ICA. Since the resistance gradient is related to lithium diffusion and polarization [30], this parameter may serve as a useful indicator for identifying the optimal external pressure to enhance anode performance.

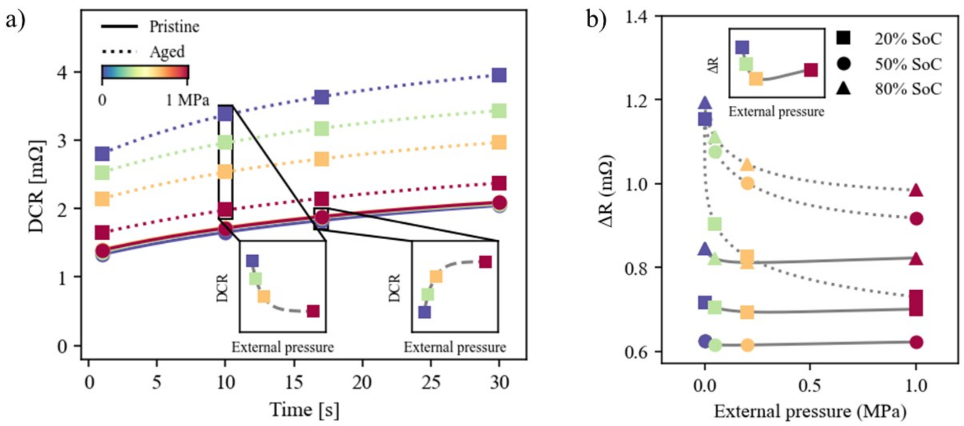

Figure 7: Impedance analysis with different initial stack pressures: a) DCR.b) Resistance gradient of the end of the pulse to the beginning.

To confirm the observed trends, Fig.8 presents the evolution of DCR for pristine cells (Fig.8a–c) and aged cells (Fig.8d–f) at 20%, 50%, and 80% SoC. Across all SoC levels, similar behaviour is observed. In pristine cells, the influence of external pressure becomes more pronounced over the duration of the pulse, suggesting a time-dependent response likely related to increasing interfacial contact or enhancing battery kinetics. In contrast, aged cells exhibit a more generalized and consistent pressure effect throughout the pulse, indicating a generalized enhancement in conductivity.

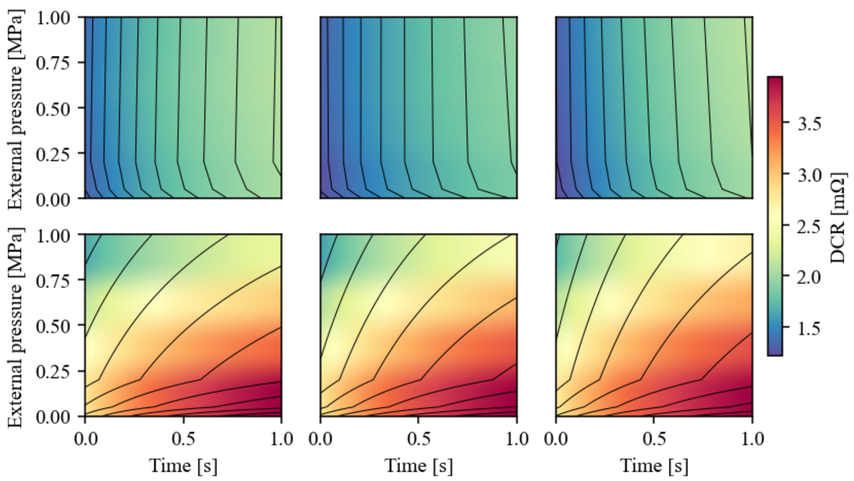

Figure 8: DCR measurements with different initial stack pressures along the pulses: a) Pristine cell with 20% SoC. b) Pristine cell with 50% SoC. c) Pristine cell with 80% SoC. d) Aged cell with 20% SoC. e) Aged cell with 50% SoC. f) Aged cell with 80% SoC.

5 Conclusions

This study demonstrated that external mechanical pressure has a measurable and varying influence on the electrochemical performance of commercial prismatic lithium-ion cells, with distinct behaviours observed between pristine and aged cells. The results show that pressure improves discharge capacity and reduces impedance, but the effects are significantly more pronounced in aged cells. As the external pressure reduces the swelling of the cell, the hypothesis is that the contact between electrodes and the electrolyte infiltration is improving as the cell recovers its initial shape [31].

For pristine cells, the effect of pressure on discharge capacity was minimal (maximum of 0.46%), while aged cells experienced up to a 2.88% improvement. Similarly, impedance measurements revealed that aged cells benefited from a substantial 41.3% decrease in ohmic resistance under 1 MPa of pressure, indicating that pressure restores or enhances conductive pathways within deteriorated internal structures due to effects such as delamination or gas generation [29]. This effect does not appear in pristine cells, where impedance slightly increases.

The ICA provided insight into the impact of pressure on electrochemical processes, particularly in relation to phase transitions in the graphite anode. In pristine cells, the graphite transition voltage initially decreased with increasing pressure before reversing, indicating an optimal pressure point around 0.2 MPa for enhanced anode kinetics. Aged cells, however, showed a continued decrease in transition voltage with pressure, suggesting altered behaviour due to aging.

The analysis of reversible swelling pressure revealed differences in the mechanical response of aged versus pristine cells, particularly in their stiffness and pressure variation during cycling. Aged cells exhibited lower mechanical stiffness at low stack pressures, likely due to gas accumulation. High external pressure helped compact the aged cells and restore some mechanical uniformity, aligning their mechanical response more closely with that of pristine cells.

This study highlights the impact of external pressure on lithium-ion cell performance, particularly in aged cells. However, its scope is limited by the use of only one pristine and one aged cell, a single aging condition, and possible temperature variations during capacity tests. Additionally, the limited number of pressure points reduces the resolution of the mechanical influence. Future work should include a larger sample size, varied aging conditions, tighter thermal control, and more external pressure conditions to strengthen the findings. Nevetheless, they highlights the role of external pressure in lithium-ion cell performance. Rather than applying a one-size-fits-all approach, pressure should be understood as a condition with variable impact depending on the cell's state of health. These insights can guide the development of more optimized battery pack designs and maintenance strategies, where applied pressure is managed not only to ensure structural integrity but also to enhance and sustain electrochemical performance over the battery's lifetime. Incorporating these findings into battery system engineering could lead to longer-lasting, more efficient energy storage solutions.

Acknowledgments

This work was supported by ELKARTEK project ELASTBAT from the Basque Government and Ikerlan Technology Research Centre.

References

[1] J. Vetter et al., *Ageing mechanisms in lithium-ion batteries*, Journal of Power Sources, ISSN 0378-7753, 147(2005), 267-281.

[2] S. Arora et al., *Review of mechanical design and strategic placement technique of a robust battery pack for electric vehicles*, Renewable and Sustainable Energy Reviews, ISSN 1364-0321, 60(2016), 1319-1331.

[3] P. Cicconi and P. Kumar, *Design approaches for Li-ion battery packs: A review*, Journal of Energy Storage, ISSN 2352-152X, 73(2023), 109197.

[4] L. Aiello et al., *Influence of Pressure, Temperature and Discharge Rate on the Electrical Performances of a Commercial Pouch Li-Ion Battery*, Batteries, ISSN 2313-0105, 10(2024), 72.

[5] S. Lv et al., *The Influence of Temperature on the Capacity of Lithium Ion Batteries with Different Anodes*, Energies, ISSN 1996-1073, 15(2022), 60.

[6] F. Leng et al., *Effect of Temperature on the Aging rate of Li Ion Battery Operating above Room Temperature*, Scientific Reports, ISSN 2045-2322, 5(2015), 12967.

[7] L. Liao et al., *Effects of temperature on charge/discharge behaviors of LiFePO4 cathode for Li-ion batteries*, Electrochimica Acta, ISSN 0013-4686, 60(2012), 269-273.

[8] S. Barcellona et al., *Aging effect on the variation of Li-ion battery resistance as function of temperature and state of charge*, Journal of Energy Storage, ISSN 2352-1538, 50(2022), 104658.

[9] X. Wang et al., *The Impact of Wide Discharge C-Rates on the Voltage Plateau Performance of Cylindrical Ternary Lithium-Ion Batteries*, Energies, ISSN 1996-1073, 17(2024), 3488.

[10] M. Metzger et al., *Carbon Coating Stability on High-Voltage Cathode Materials in H 2 O-Free and H 2 O-Containing Electrolyte*, Journal of The Electrochemical Society, ISSN 1945-7111, 162(2015), 1227-1235.

[11] H. Raj et al., *Effect of carbon coating on electrochemical performance of LiFePO4 cathode material for Li-ion battery*, Ionics, ISSN 0947-7047, 24(2018), 26.

[12] G. Gonzaga dos Santos et al., *Effect of ambient temperature, C-rate and SOH on the charge and discharge performance and self-temperature of LCO batteries*, International Journal for the Joining of Materials, ISSN 0905-6866, 9(2021), 1-11.

[13] L. Chen et al., *Estimation the internal resistance of lithium-ion-battery using a multi-factor dynamic internal resistance model with an error compensation strategy*, Energy Reports, ISSN 2352-4847, 7(2021), 3050-30.

[14] J. Zhu et al., *Studies on the medium-frequency impedance arc for Lithium-ion batteries considering various alternating current amplitudes*, Journal of Applied Electrochemistry, ISSN 1572-8838, 46(2016), 157–167.

[15] X. Wang et al., *State Estimation of Lithium Ion Battery Based on Electrochemical Impedance Spectroscopy with On-Board Impedance Measurement System*, IEEE Vehicle Power and Propulsion Conference (VPPC), ISSN 2769-4186, (2015), 1-5.

[16] B. Xu et al., *Decoupling the thermal and non-thermal effects of discharge C-rate on the capacity fade of lithium-ion batteries*, Journal of Power Sources, 0378-7753, 510(2021), 230390.

[17] X. Du et al., *Characterization and analysis of the effect of pressure on the performance of a large format NMC/C lithium-ion battery*, Journal of Power Sources, ISSN 0378-7753, 573(2023), 233117.

[18] V. Muller et al., *Study of the influence of mechanical pressure on the performance and aging of Lithium-ion battery cells*, Journal of Power Sources, ISSN 0378-7753, 440(2019), 227148.

[19] Y. Jiang et al., *Effects of stack pressure on the equivalent circuit model of lithium-ion batteries*, Journal of Energy Storage, ISSN 2352-152X, 70(2023), 107916.

[20] L. Zhou et al., *A study of external surface pressure effects on theproperties for lithium-ion pouch cells*, International Journal of Energy Research, ISSN 0363-907X, 44(2020), 6089-7103.

[21] X. Wang et al., *Influence of Different Ambient Temperatures on the Discharge Performance of Square Ternary Lithium-Ion Batteries*, Energies, ISSN 1996-1073, 15(2022), 5348.

[22] X. Cai et al., *Characterization and quantification of multi-field coupling in lithium-ion batteries under mechanical constraints*, Journal of Energy Chemistry, ISSN 2095-4956, 95(2024), 364-379.

[23] A. Mussa et al., *Effects of external pressure on the performance and ageing of single-layer lithium-ion pouch cells*, Journal of Power Sources, ISSN 0378-7753, 385(2018), 18-25.

[24] A. Avdyli et al., *Modeling and Experimental Investigation of the Interaction between Pressure-Dependent Aging and Pressure Development Due to the Aging of Lithium-Ion Cells*, Batteries, ISSN 2313-0105, 9(2023), 484.

[25] W. Li et al., *Clarifying the Effect of Pressure on Performance in Lithium-Ion Batteries*, Journal of The Electrochemical Society, ISSN 0013-4651, 172(2025), 010512.

[26] J. Koo et al., *Detrimental electrochemical behavior caused by excessive high pressure on Li-ion pouch-type full cell*, Electrochemistry Communications, ISSN 1388-2481, 152(2023), 107518.

[27] M. Wünsch et al., *Investigation of the influence of different bracing of automotive pouch cells on cyclic liefetime and impedance spectra*, Journal of Energy Storage, ISSN 2352-1538, 21(2019), 149-155.

[28] T. Pathan et al., *Active formation of Li-ion batteries and its effect on cycle life*, JPhys Energy, ISSN 2515-7655, 1(2019), 044003).

[29] K. Büscher et al., *The Beneficial Effect of Pressure for Lithium Ion Battery Cells through Gas Dissipation*, Journal of The Electrochemical Society, ISSN 1945-7111, 171(2024), 090532).

[30] J. Kim et al., *Principles and Applications of Galvanostatic Intermittent Titration Technique for Lithium-ion Batteries*, Journal of Electrochemical Science and Technology, ISSN 2288-9221, 13(2022), 19-31).

[31] A. Chahbaz et al., *Pressure-Induced Capacity Recovery and Performance Enhancements in LTO/NMC-LCO Batteries*, Advanced Functional Materials, ISSN 1616-301X, 1(2025), 1616-3028).

Presenter Biography

Ander Avila received his M.Sc. in Industrial Engineering from the University of Mondragon, in 2023 and his M.Sc. in Mechanics of Materials and Structures from University of Girona, in 2024. He joined the Mechatronic unit of Ikerlan Technology Research Centre, Spain, in 2021. He started working on the design criteria of lithium-ion battery packs. Then, he focused his work in 2023 in the mechanical phenomena of battery cells. His research interests include coupling of mechanical effects in lithium-ion batteries with their performance and degradation. He is currently coursing his Ph.D. in Applied Engineering in collaboration with Ikerlan Technology Research Centre and University of Girona.